Technical Physics, Vol. 49, No. 7, 2004, pp. 843–848. Translated from Zhurnal Tekhnicheskoĭ Fiziki, Vol. 74, No. 7, 2004, pp. 38–43.

GAS DISCHARGES, PLASMA

Study of Metal Conductivity near the Critical Point Using a Microwire Electrical Explosion in Water

V. I. Oreshkin[1]*, R. B. Baksht[1], A. Yu. Labetsky[1], A. G. Rousskikh[1], A. V. Shishlov[1], P. R. Levashov[2], K. V. Khishchenko[2], and I. V. Glazyrin[3]*****

[1]*Institute of High Current Electronics, Siberian Division, Russian Academy of Sciences, Akademicheskiĭ pr. 4, Tomsk, 634055 Russia*

** e-mail: oreshkin@ovpe.hcei.tsc.ru*

[2]*Institute for High Energy Densities, Russian Academy of Sciences, Izhorskaya ul. 13/19, Moscow, 125412 Russia*

*** e-mail: konst@ihed.ras.ru*

[3]*Zababakhin Institute of Technical Physics, Snezhinsk, Chelyabinskaya oblast, 456770 Russia*

**** e-mail: i.v.glazyrin@vniitf.ru*

Received December 1, 2003

Abstract—Electrical explosion of aluminum and tungsten microwires in water was studied both experimentally and numerically. The experimental range of currents through the wire was 0.1–1 kA for explosion times of 40–300 ns and current densities up to 1.5×10^8 A/cm^2. The experimental results were interpreted on the basis of magnetohydrodynamical simulation with various metal conductivity models. A comparison of the experimental and numerical results allows the conclusion to be drawn that the metal conductivity models used in this work are adequate. *© 2004 MAIK "Nauka/Interperiodica".*

INTRODUCTION

Wire electrical explosion (WEE) has drawn the attention of researchers for a long time [1]. On the one hand, WEE is of interest as an object of basic research, because the thermodynamic parameters in the exploding wire substance reach their extreme values. On the other hand, exploding wires are widely used in various technical applications, e.g., for sharpening electrical power in a high-voltage pulse technique [2]; for preparing nanopowders [3]; and as high-power sources of soft X-rays in multiwire liners [4, 5]. Traditionally, the WEE process is simulated using magnetohydrodynamic (MHD) approximation. Numerical calculations in this approximation require preliminary knowledge of the equations of state (EOS's) for a substance over a wide range of thermodynamic parameters, as well as knowledge of the transport coefficients, of which the electrical conductivity is the most important. Whereas the thermodynamic properties of metals can be described by a variety of semiempirical models and using various databases, the problems associated with the transport coefficients in the region of metal–insulator transition and in the vicinity of the critical point are less well understood. On the one hand, the WEE experiments and the MHD simulation of explosion provide information about the conductivity of a substance of interest and, on the other, they allow one to judge the adequacy of a particular conductivity model. From this point of view, of greatest interest is the WEE in a liquid dielectric, in particular, in water, rather than in vacuum, where WEE is accompanied by such phenomena as stratification, gas desorption from wire surface, etc., which are not directly related to the transport properties of a conductor [6].

As is known [2], at the initial (heating) WEE stage, the parameters of a metal substance move along the liquid branch of a binodal, i.e., along the boundary between the condensed and two-phase (vapor–liquid mixture) states. As for the wire explosion, it happens in the vicinity of a critical point, i.e., a point where distinction between the liquid and gas phases disappears. For this reason, knowledge of the dependence of metal conductivity near the critical point on the energy input rate into the wire substance is of prime importance in the WEE simulation. Indeed, the substance in this two-phase region of the phase diagram is a mixture of vapor and the drop fraction of liquid metal, while it is the energy input rate which determines the size of the drop fraction. Moreover, metal in this region can be in the metastable state, i.e., be a superheated liquid, whose conductivity may strongly differ from the conductivity of the vapor–drop mixture. The relaxation times in the transition of a superheated metal to the vapor–drop mixture lie in the range 1–10 ns. For this reason, we used the same conductivity models in the WEE simulation both for the microsecond current- growth regime, where the metastable metal states do not play any significant role, and for the nanosecond regime.

1063-7842/04/4907-0843$26.00 © 2004 MAIK "Nauka/Interperiodica"

In this work, an electrical explosion of aluminum and tungsten wires in water was studied experimentally and numerically for different energy-input regimes and different current-growth times. The purpose of this work was to estimate the metal conductivity in the vicinity of the critical point. The experimental results were compared with the results of MHD simulation, which was carried out using different methods for the description of the thermophysical properties of the medium. Agreement between the experimental results and the results of MHD simulation of the microwire electrical explosion is taken as a criterion for the validity of the estimates obtained for metal conductivity near the critical point.

EXPERIMENTAL

Experiments were carried out with a current generator schematically illustrated in Fig. 1. It was an *LC* circuit consisting of a capacitor bank with capacity C = 0.067 μF assembled from IKCh-50-0.035 capacitors. The bank discharged into a load trough a controlled gas-filled gap and inductance L. The inductance L was a plug-in solenoid; in the experiments, it had either of two values 2.25 and 0.73 μH, allowing the wire explosion to be carried out in various current-growth regimes. The circuit resistances R in these two regimes were 0.47 and 0.35 Ω, respectively (without regard for the microwire resistance). The load unit was placed inside the generator operating chamber. Six rods with a diameter of 1 cm uniformly arranged along a circle of diameter 10 cm were used as a return wire. A rodlike return wire was chosen to minimize the stray capacitance of the load unit. The water resistivity in the experiments was no worse than 150 kΩ cm. After each shot, water was renewed, purified, and deionized.

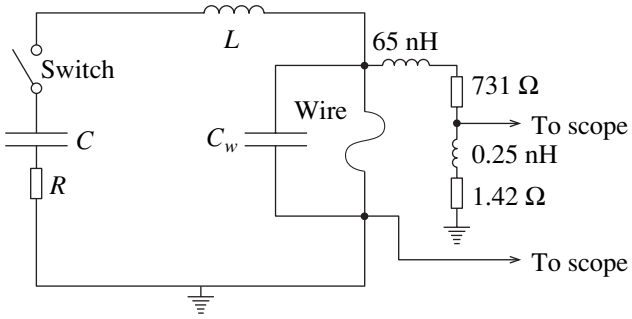

Fig. 1. Electric scheme of the experimental setup.

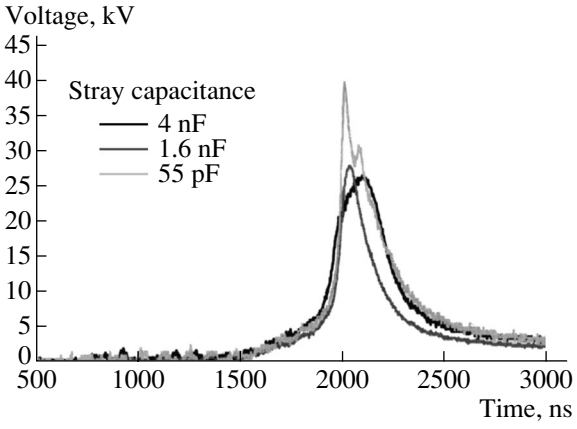

Fig. 2. Voltage oscillograms of wire explosions for different stray capacitances.

The following electrophysical diagnostics were used in the experiments: a high-ohmic divider, an inductance loop placed on the side of a high-voltage electrode (anode), and a shunt placed on the side of a grounded electrode (Fig. 1).

The load impedance is the sum of the microwire impedance consisting of the ac ohmic and inductive wire resistances and the reactance of the interelectrode-gap stray capacitance C_w. Upon an abrupt change in the bias on the gap, a portion of current goes to charging the stray capacitor. As a result, the time dependence of current measured on the side of high-voltage electrode differs from the time dependence of current measured on the grounded electrode. Since the voltage derivative at the instant of wire explosion can be very high, the presence of a stray capacitance of several picofarads can result in a considerable current loss and a decrease in the detected peak voltage. Such a measurement error may lead to an incorrect interpretation of the results obtained. We performed several test microwire explosions with different values of stray capacitance (Fig. 2). It becomes clear from the oscillograms shown in this figure that the gauge indications are related to the stray capacitance. In our experiments, the capacitance of the interelectrode gap was minimized to C_w = 55 pF. This value of stray capacitance was included in the scheme of the electric circuit used in our calculations.

MAGNETOHYDRODYNAMIC MODEL

The electrical explosion process was simulated within the framework of a single-temperature magnetohydrodynamic approximation. For the cylindrical geometry, the MHD equations have the form

$$\frac{d\rho}{dt} + \frac{\rho}{r}\frac{\partial v}{\partial r} = 0; \quad (1)$$

$$\rho\frac{dv}{dt} = -\frac{\partial \rho}{\partial r} - j_z B_\varphi; \quad (2)$$

$$\rho\frac{d\varepsilon}{dt} = -\frac{p}{r}\frac{\partial v}{\partial r} + \frac{j_z^2}{\sigma} + \frac{1}{r}\frac{\partial}{\partial r}\left(\kappa\frac{\partial T}{\partial r}\right); \quad (3)$$

$$\frac{1}{c}\frac{\partial B_\varphi}{\partial t} = \frac{\partial E_z}{\partial r}; \quad j_z = \frac{c}{4\pi r}\frac{\partial (rB_\varphi)}{\partial r}; \quad (4)$$

$$j_z = \sigma E_z; \quad (5)$$

$$\varepsilon = f(\rho, T); \quad p = f(\rho, T), \tag{6}$$

where

$$\frac{d}{dt} = \frac{\partial}{\partial t} + v\frac{\partial}{\partial r}$$

is the substantial derivative; ρ and T are the substance density and temperature, respectively; v is the velocity radial component; p and ε are the pressure and the internal energy, respectively; B_φ is the azimuthal component of magnetic field; E_z is the axial component of electric field; j_z is the axial component of current density; and κ and σ are the thermal conductivity coefficient and the conductivity, respectively.

Equations (1)–(6) were solved numerically using a one-dimensional MHD code [7] written in the Lagrange coordinates. With this code, hydrodynamical Eqs. (1)–(3) were solved using the explicit difference scheme "cross" [8] with a combined pseudoviscosity (linear and quadratic) introduced for the calculation of shock waves. Maxwell Eqs. (4) complemented by Ohm's law (5) and the heat conduction equation were solved using implicit difference schemes based on the data-flow sweep method [9]. In the numerical simulation of the WEE in water, the computational grid consisted of two regions: the conducting substance and water. It was assumed that the water conductivity is zero, so that the current flows only in metal, while the shock wave propagates in water.

The boundary condition for the Maxwell equations was written as

$$B_\varphi(R) = \frac{2I_n}{cR}, \tag{7}$$

where R is the wire outer radius and I_n is the current flowing through the wire.

The current flowing through the wire was determined from the joint solution to the Maxwell equations and the system of equations of electric circuit presented in Fig. 1. The stray capacitance in the electric circuit was also taken into account.

The system of MHD equations is closed by the EOS (6) for the substance. The wide-range EOS's [10, 11] obtained on the basis of a semiempirical model [10] were used for metal. The EOS model [10] allows for the high-temperature melting and evaporation effects, and the special form [1] of the EOS tables can take into account the metastable states of the liquid and gas phases on the phase diagram. The EOS's were used for water [12].

The electrical conductivity of aluminum was calculated by two methods. In the first of them, it was determined from the conductivity tables [13] compiled by M. Desjarlais at the Sandia National Laboratories (USA) on the basis of the model [14] modified with allowance for the experimental data. In the second method, the conductivity was determined by the combined computational and experimental procedure [15], in which the conductivity is considered as a certain empirical function of the density and specific energy deposited in a substance. With this method, the conductivity parametrically depends on the particular form of the EOS.

The conductivity tables in this method are constructed using the following initial data: (1) the tabulated normal-density dependence $\sigma_1(T, \delta = 1)$ and (2) the conductivity in the gas–plasma region calculated by the classical formulas [16]. In the transition region near the critical point, the conductivity is taken in the parametric form [15], which we have modified by the introduction of a new parameter γ that was set equal to unity in [15]:

$$\log\frac{\sigma(T, \delta)}{\sigma_1(T, \delta = 1)} = \Phi(T, \delta)\log\frac{\sigma_{cr}}{\sigma_1}\left(\frac{\log\delta}{\log\delta_{cr}}\right)^\gamma, \tag{8}$$

where σ_{cr} is the conductivity at the critical point; $\delta = \rho/\rho_0$ is the relative density of the substance; ρ_0 is its normal density; δ_{cr} is the relative density at the critical point; and $\Phi(T, \delta)$ is a function, on the order of unity, depending on the position of the interface in a mixture of phases.

When constructing the conductivity tables, the value of σ_{cr} is a variable parameter, and it is assumed to be independent of temperature. The critical conductivity is chosen in such a way as to provide the best agreement between the results of MHD simulation and the totality of experimental data.

A comparison of the tables of aluminum conductivity [13] with the corresponding tables constructed using the procedure in [15] demonstrates a good agreement between them, both qualitative and quantitative. Since we lacked data on the electrical conductivity of tungsten like those for aluminum in [13], the MHD calculations were carried out using tables constructed by the computational and experimental procedure described in [15]. In this case, the value of parameter γ was chosen to be 2.2, in contrast to aluminum, for which we took $\gamma = 1$, as in [15].

COMPARISON AND DISCUSSION OF THE EXPERIMENTAL AND COMPUTATIONAL RESULTS

The experiments on electrical explosion and the MHD calculations were carried out for aluminum and tungsten microwires of different diameter. In the experiments, the current through the wire and the voltage on the wire were measured; the same quantities were calculated in the numerical simulation of electrical explosion. The current through the load unit was also calculated as the sum of the current through the wire and the displacement current flowing through the water stray capacitance. The comparison of the computational and experimental time dependences of current and voltage

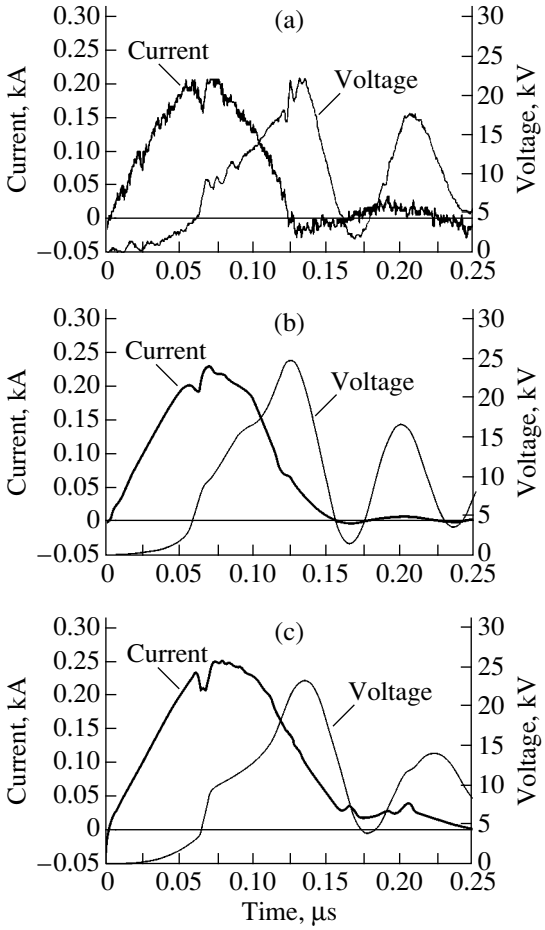

Fig. 3. (a) Experimental and (b, c) calculated time dependences of current and voltage for the explosion of aluminum wire in the regime $L = 2.25$ μH and $U_0 = 10$ kV. Calculations with the electrical conductivity from (b) [13] and (c) [15].

suggests that the conductivity models and the EOS used in the calculations were adequate.

In Fig. 3a, the experimental oscillograms of the current through the sample and the voltage on it are presented for the explosion of an aluminum wire 15 μm in diameter and 2.6 cm in length in a circuit with parameters $L = 2.25$ μH and $U_0 = 10$ kV. One can see in this figure that the current through the wire drops virtually to zero almost immediately after the voltage maximum. In other words, the discharge channel disappears. The oscillations detected by the current and voltage gauges are caused by the recharging of the stray capacitance C_w. The calculated time dependences of the current through the microwire and the voltage on the interelectrode gap are shown in Fig. 3b. For this case, the calculations were carried out using the EOS from [10] and conductivity tables from [13]. One can see in this figure that the experimental and calculated curves coincide well with each other. Both the instants of explosion and the voltage amplitudes coincide. In addition, the instant of wire melting is seen at ~60 ns in both figures. The voltage maxima after the explosion are caused by the recharging of the stray capacitance C_w.

The current and voltage time dependences calculated for the same regime using the EOS from [10] and the conductivity tables constructed by the procedure [15] are shown in Fig. 3c. One can see from a comparison of Figs. 3a and 3c that the agreement between the experimental and calculated curves is good in this case as well. As in the case with the use of the conductivity tables from [13], the instant of explosion and the voltage amplitude are described here with rather good accuracy. This is caused by the fact that both the character of the change in metal conductivity and its absolute value in models [13] and [15] approximately coincide in the time interval from the condensed state to the critical density. For example, the aluminum critical conductivity determined using the procedure [15] is $\sigma_{cr} = 2.8 \times 10^3\ \Omega^{-1}\ cm^{-1}$. The difference between this value and the values of conductivity in table [13] does not exceed 40% in the temperature range from room to ~3 eV (which is almost fivefold higher than the critical temperature). At higher temperatures, the discrepancy is greater, and, at temperatures on the order of 100 eV, the critical conductivity acquires a plasma character. However, for wire explosions in the region of near-critical densities, temperatures as high as those are not achieved.

Notice that the calculations were carried out both with and without allowance for the possible occurrence of the metastable metal states. However, the inclusion of such states had only a small effect on the current–voltage characteristics of the wire electrical explosion. The distinction between the results proved to be equal to tenths of one percent (the experimental accuracy was appreciably worse). The effect of liquid-phase superheating on the density distribution along the wire radius proved to be considerably stronger, as was already pointed out in [11].

The experimental data and their comparison with the calculations are summarized in Table 1. The five-shot-averaged values of maximal current, maximal voltage, and the explosion time measured as the time interval from zero to the voltage maximum are given in the table. The calculations were carried out with the values of conductivity obtained using the computational and experimental procedure [15]. One can see that the error of calculation comprises about 20% over a rather wide range of parameters.

When simulating the electrical explosion of tungsten wires, we used the conductivity tables constructed by procedure [15]. The tungsten critical parameters are appreciably different from those of aluminum. For instance, $\rho_{cr} = 4.85$ g/cm^3 and $T_{cr} = 1.36$ eV for tungsten and $\rho_{cr} = 0.64$ g/cm^3 and $T_{cr} = 0.67$ eV for aluminum. At the same time, the critical conductivities of these substances differ only slightly; for tungsten, $\sigma_{cr} = 2.6 \times 10^3\ \Omega^{-1}\ cm^{-1}$.

Table 1. Comparison of the experimental and calculated parameters for the explosion of aluminum wires with a diameter of 15 μm and a length of 2.6 cm

Inductance, nH	Charging voltage, kV	Explosion time, ns		Explosion voltage, kV		Maximal current, A	
		experiment	calculation	experiment	calculation	experiment	calculation
2251	10		124	20.7	24.7	200	230
2251	20	80	81	42	54.8	273	305
730	20	48	45.1	28.9	39	383	450

Table 2. Comparison of the experimental and calculated parameters for the explosion of tungsten wires with a diameter of 30 μm and a length of 2 cm

Inductance, nH	Charging voltage, kV	Explosion time, ns		Explosion voltage, kV		Maximal current, A	
		experiment	calculation	experiment	calculation	experiment	calculation
2251	10	471	434	15.5	12	417	482
2251	20	239	230	33.3	37.3	607	671
2251	30	167	175	44	60	805	853
730	10	369	389	10.8	10.1	541	646
730	20	169	160	26.5	25.6	735	832
730	30	113	105	41	51	970	1100

In Fig. 4a, the oscillograms of the current through the wire and the voltage on it in the explosion regime are shown for a tungsten wire with a diameter of 30 μm and a length of 2 cm in a circuit with $L = 0.73$ μH and $U_0 = 20$ kV. The corresponding calculated time dependences are shown in Fig. 4b. The agreement between the experimental and calculated curves in the case of tungsten wires is seen to be somewhat worse than for aluminum. In particular, the first maximum corresponding to metal melting is more pronounced in the calculated voltage curve than in the experimental curve. However, the absolute value and the time of the second maximum, which we assign to the instant of explosion, coincide rather well. At the instant of explosion, the resistance increases drastically, and the thermodynamic parameters of the wire substance are close to their values at the critical point; i.e., the temperature is 1–1.5 eV and the density is 2–6 g/cm^3.

The experimental data on the explosion of tungsten wires and the comparison with the corresponding calculations are summarized in Table 2. As before, five shots were made for each set of parameters. The calculations were carried out with the conductivities obtained by the computational and experimental procedure [15]. One can see that the error of calculation is no worse than for aluminum and does not exceed 20% over a rather wide range of parameters.

To check the applicability of the tables of tungsten conductivity for the description of wire explosions in the microsecond current-growth regime, the explosion of tungsten wire was simulated for the experimental conditions described in [17]. In those experiments, the current generator was also an *LC* circuit with parameters $C = 6$ μF, $L = 4.5$ μH, and $U_0 = 20$ kV. The wires were 0.35 mm in diameter and 8.7 cm in length, and they were also exploded in water. The results of the simulation are presented in Fig. 5. The solid curves are for the calculated time dependences of current and voltage, and the marks are the experimental values of these

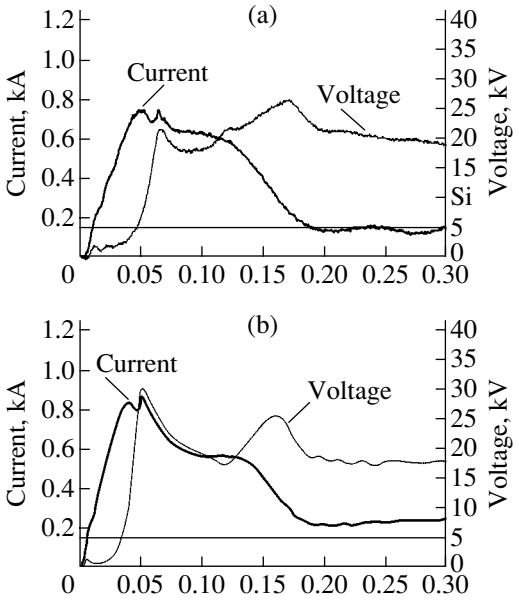

Fig. 4. (a) Experimental and (b) calculated time dependences of current and voltage for the explosion of tungsten wire in the regime $L = 0.73$ μH and $U_0 = 20$ kV.

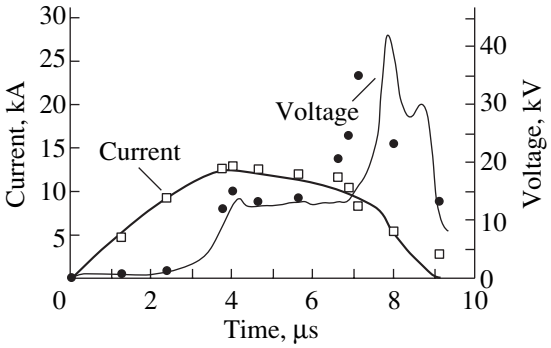

Fig. 5. Experimental (□ current, ● voltage) and calculated (solid lines) time dependences of current and voltage for the microsecond explosion of tungsten wire.

quantities. One can see that, although the tables of tungsten conductivity were constructed on the basis of the experiments on wire explosion in the nanosecond current-growth regimes, they satisfactorily describe wire electrical explosion in regimes with current-growth times longer by almost three orders of magnitude. The calculated curves coincide well with the experimental ones both in explosion time and in voltage amplitude; the discrepancy between the calculated and experimental quantities is less than 10%. This is evidence that the tungsten conductivity in the electrical explosion is independent of the rate of energy input into the substance.

CONCLUSIONS

Thus, a wire electrical explosion in water can be described rather well within the framework of magnetic hydrodynamics. The experimental data on WEE in liquid dielectrics are the source of information on the metal conductivity near the critical point. The coincidence of the experimental data with the results of MHD simulation of the WEEs with substantially different current-growth times suggests that metal conductivity near the critical point is a function of the state of the substance (temperature and density) and is independent of the energy-input rate.

ACKNOWLEDGMENTS

We are grateful to M. Desjarlais for providing the tables of aluminum conductivity and to N.A. Ratakhin and S.I. Tkachenko for discussions. This work was supported by the ISTC (grant no. 1826) and RFBR (grant no. 04-02-17292).

REFERENCES

1. *Exploding Wires*, Ed. by W. G. Chace and H. K. Moore (Plenum, New York, 1959; Mir, Moscow, 1965).
2. V. A. Burtsev, N. V. Kalinin, and A. V. Luchinskiĭ, *Electric Explosion in Conductors and Its Electrophysical Applications* (Énergoatomizdat, Moscow, 1990).
3. V. S. Sedoy, G. A. Mesyats, V. I. Oreshkin, *et al.*, IEEE Trans. Plasma Sci. **27**, 845 (1999).
4. S. A. Pikuz, T. A. Shelkovenko, J. B. Greenly, *et al.*, Phys. Rev. Lett. **83**, 4313 (1999).
5. R. B. Spielman, C. Deeney, G. A. Chandler, *et al.*, Phys. Plasmas **5**, 2105 (1998).
6. A. M. DeSilva and J. D. Katsouros, Phys. Rev. E **57**, 5945 (1998).
7. V. I. Oreshkin, V. S. Sedoĭ, and L. I. Chemezova, Prikl. Fiz., No. 3 (2001).
8. N. N. Kalitkin, *Numerical Methods* (Nauka, Moscow, 1978).
9. A. A. Samarskiĭ and Yu. P. Popov, *Difference Schemes in Gas Dynamics* (Nauka, Moscow, 1975).
10. A. V. Bushman and V. E. Fortov, Sov. Technol. Rev. B **1**, 219 (1987).
11. S. I. Tkachenko, K. V. Khishchenko, V. S. Vorob'ev, *et al.*, Teplofiz. Vys. Temp. **39**, 728 (2001) [High Temp. **39**, 674 (2001)].
12. A. T. Sapozhnikov, G. V. Kovalenko, P. D. Gershchuk, *et al.*, Vopr. At. Nauki Tekh., Ser.: Mat. Model. Fiz. Protsessov, No. 2, 15 (1991).
13. M. P. Desjarlais, Contrib. Plasma Phys. **41**, 267 (2001).
14. Y. T. Lee and R. M. More, Phys. Fluids **27**, 1273 (1984).
15. Yu. D. Bakulin, V. F. Kuropatenko, and A. V. Luchinskiĭ, Zh. Tekh. Fiz. **46**, 1963 (1976) [Sov. Phys. Tech. Phys. **21**, 1144 (1976)].
16. N. N. Kalitkin, Preprint No. 85, IPM (Institute of Applied Mathematics, Moscow, 1978).
17. N. I. Kuskova, S. I. Tkachenko, and S. V. Koval, J. Phys.: Condens. Matter **9**, 6175 (1997).

Translated by V. Sakun